Vietnam Journal of Mechanics, Vol. 46, No. 3 (2024), pp. 265 – 281
DOI: https://doi.org/10.15625/0866-7136/21064

VIBRATION OF AGGLOMERATED CNTRC MICRO-SCALE BEAMS CARRYING A MOVING CONCENTRATED LOAD

Thi Thom Tran*, Dinh Kien Nguyen
Institute of Mechanics, VAST, 18 Hoang Quoc Viet, Hanoi, Vietnam
*E-mail: ttthom@imech.vast.vn

Received: 15 March 2024 / Revised: 15 August 2024 / Accepted: 26 August 2024
Published online: 14 September 2024

Abstract. Vibration of micro-scale composite beams reinforced by carbon nanotubes (CNTRC beams) carrying a moving concentrated load is studied considering CNT agglomeration. The Eshelby–Mori–Tanaka method is adopted to predict the elastic moduli of the CNTRC. The modified couple stress theory and a refined high-order theory are employed to establish the mathematical model. The governing equation in terms of finite element analysis is established and solved by a direct integration method. The effects of the CNT reinforcement, the agglomeration of CNTs, the size scale parameter, and the load speed on the vibration of the beams are investigated in detail.

Keywords: CNTRC, agglomeration, micro-scale beam, vibration, FEM.

1. INTRODUCTION

Carbon nanotubes (CNTs) with the combination of high surface ratio, ultra-lightweight, and high mechanical strength make them materials with diverse application potential. One of them is excellent reinforcement for composite materials. However, CNTs have a very high aspect ratio and low stiffness in bending, CNT agglomeration can occur within a polymeric matrix. To consider the agglomeration effect on the properties of CNT composites, a two-parameter micromechanical model was proposed by Shi et al. [1], and this model was employed to CNT-reinforced composite (CNTRC) structures. Heshmati and Yas [2] used the two-parameter model in combination with the Mori–Tanaka (M-T) scheme to determine the effective properties of randomly oriented CNTRC beams. The authors concluded that the CNT agglomeration exerts a significant

weakening effect in the composites. Most recently, Tran and Nguyen [3] studied the dynamics of sandwich CNTRC inclined beams traversed by a moving mass, considering the CNT agglomeration. From the numerical investigations, the authors concluded that the CNT agglomeration has a significant impact on the beam dynamics, and the agglomeration should not be ignored in the dynamic analysis of the CNTRC beam structure.

It has been shown that the small size effect is important in predicting the response of micro-scale structural elements. In order to capture the size effect, various continuum theories, such as the couple stress elasticity, nonlocal elasticity, strain gradient elasticity, and surface elasticity have been proposed for studying the mechanical behavior of micro-scale structures [4]. The couple stress theory with two classical and two additional material constants was proposed in [5, 6] for isotropic elastic solids. However, the determination of the two constants in the theory is very difficult, and this limits its applications. To amend this limitation, Yang et al. [7] proposed the so-called modified couple stress theory (MCST), which requires one additional material scale parameter only. Using MCST, Mohammadimehr et al. [8] presented the vibration analysis of a micro-scale composite beam reinforced by single-walled carbon nanotubes (SWCNTs), considering four types of CNT distribution. It has been shown that the microcomposite beam moves toward greater stability when increasing the size scale parameter. Free vibration of CNTRC microbeams was explored by Civalek et al. [9], also considering four types of CNT distribution in the polymeric matrix. The microstructure-dependent differential equations are derived in the basis of MCST, and then solved via the Navier solution. The MCST was employed in combination with Euler–Bernoulli and Timoshenko beam theories by Al-Shewailiah and Al-Shujairi [10] to study the bending of FG-SWCNTRC microbeams, considering the porosities. It is worth noting that CNT agglomeration was not considered in Refs. [8–10]. Recently, the Timoshenko beam theory and the MCST were adopted by Esen [11] to explore the moving load problem of micro-scale homogeneous microbeams under a moving load. The finite element method (FEM) is used by the author to predict the dynamic response of the microbeam.

In this paper, the vibration of micro-scale CNTRC beams carrying a moving concentrated load is studied, considering the effect of CNT agglomeration. The effective elastic properties of the beam are estimated by the M-T approach (also known as the Eshelby–Mori–Tanaka model). The basis equations for the microbeams are derived on the basis of the MCST and a refined higher-order beam theory. A novel beam element is derived and employed to construct the discretized governing equation. Vibration characteristics are predicted using a direct integration method. The influence of the CNT reinforcement, the agglomeration of CNTs, the scale parameter and the load parameter on the vibration is investigated.

2. MATHEMATICAL MODEL FORMULATION

2.1. Micro-scale CNTRC beam under a moving concentrated load

A simply supported (S-S) microbeam reinforced by SWCNTs with length L, section $(b \times h)$, carrying a concentrated load P is considered. The microbeam is placed in a Cartesian system (x, z) with the x-axis being on the mid-plane, and the z-axis directs upward.

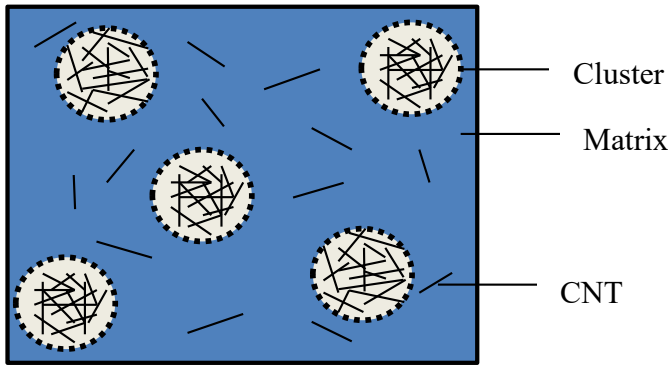

Fig. 1. Distribution of CNTs in RVE

Following the two-parameter model by Shi [1], we consider a representative volume element (RVE), V, with the non-uniform distribution of CNTs as shown in Fig. 1. There are more concentrated CNT domains, and Shi [1] assumed those domains to be spherical in shape, or considered as clusters, and of course the material properties in them are also different from the surrounding regions. Some concepts are included as follows: $V^{cluster}$ denotes the volume of clusters in the RVE, V_r is the total volume of CNTs in the RVE, $V_r^{cluster}$ and V_r are the volumes of CNTs inside the clusters and in the polymer matrix, respectively. So, we will have

$$V_r = V_r^{cluster} + V_r.$$

Two agglomeration parameters are introduced to evaluate the degree of convergence of CNTs

$$\xi = \frac{V^{cluster}}{V}, \quad \zeta = \frac{V_r^{cluster}}{V_r}, \quad 0 \leq \xi, \quad \zeta \leq 1.$$

Let the volume fraction of CNT in the composite be $V_{CNT} = V_r/V$ and assume that CNTs are transversely isotropic. The effective bulk modulus K_{in} and the shear modulus G_{in} of the clusters, and those of the matrix K_{out}, G_{out} are calculated as follows [1]

$$
\begin{aligned}
K_{in} &= K_m + \frac{V_{CNT}\zeta\left(\delta_r - 3K_m\alpha_r\right)}{3\left(\xi - V_{CNT}\zeta + V_{CNT}\zeta\alpha_r\right)},\\
G_{in} &= G_m + \frac{V_{CNT}\zeta\left(\eta_r - 2G_m\beta_r\right)}{2\left(\xi - V_{CNT}\zeta + V_{CNT}\zeta\beta_r\right)},\\
K_{out} &= K_m + \frac{V_{CNT}\left(1-\zeta\right)\left(\delta_r - 3K_m\alpha_r\right)}{3\left[1-\xi - V_{CNT}\left(1-\zeta\right) + V_{CNT}\left(1-\zeta\right)\alpha_r\right]},\\
G_{out} &= G_m + \frac{V_{CNT}\left(1-\zeta\right)\left(\eta_r - 2G_m\beta_r\right)}{2\left[1-\xi - V_{CNT}\left(1-\zeta\right) + V_{CNT}\left(1-\zeta\right)\zeta\beta_r\right]},
\end{aligned}
\tag{1}
$$

with

$$
\begin{aligned}
\alpha_r &= \frac{3\left(K_m + G_m\right) + k_r - l_r}{3\left(G_m + k_r\right)},\\
\delta_r &= \frac{1}{3}\left[n_r + 2l_r + \frac{\left(2k_r + l_r\right)\left(3K_m + 2G_m - l_r\right)}{G_m + k_r}\right],\\
\beta_r &= \frac{1}{5}\left(\frac{4G_m + 2k_r + l_r}{3\left(G_m + k_r\right)} + \frac{4G_m}{G_m + p_r} + \frac{2\left[G_m\left(3K_m + G_m\right) + G_m\left(3K_m + 7G_m\right)\right]}{G_m\left(3K_m + G_m\right) + m_r\left(3K_m + 7G_m\right)}\right),\\
\eta_r &= \frac{1}{5}\left[\frac{2}{3}\left(n_r - l_r\right) + \frac{8G_m p_r}{G_m + p_r} + \frac{8m_r G_m\left(3K_m + 4G_m\right)}{3K_m\left(m_r + G_m\right) + G_m\left(7m_r + G_m\right)} + \frac{\left(2k_r - l_r\right)\left(2G_m + l_r\right)}{3\left(G_m + k_r\right)}\right].
\end{aligned}
\tag{2}
$$

In Eqs. (1) and (2), $K_m = \dfrac{E_m}{3\left(1-2v_m\right)}, G_m = \dfrac{E_m}{2\left(1+v_m\right)}$ are, respectively, the bulk and shear moduli of the polymer matrix. The subscripts m and r stand for the polymer and CNT reinforcement; k_r, l_r, m_r, n_r, p_r denote the Hill elastic constants of CNTs. The effective elastic moduli K and G of the composite estimated by the M-T homogenization method are as follows [1]

$$
K = K_{out}\left(1 + \frac{\xi\left(\dfrac{K_{in}}{K_{out}} - 1\right)}{1 + \alpha\left(1-\xi\right)\left(\dfrac{K_{in}}{K_{out}} - 1\right)}\right),\quad
G = G_{out}\left(1 + \frac{\xi\left(\dfrac{G_{in}}{G_{out}} - 1\right)}{1 + \beta\left(1-\xi\right)\left(\dfrac{G_{in}}{G_{out}} - 1\right)}\right),
$$

where $\alpha = \dfrac{1+v_{out}}{3\left(1-v_{out}\right)}, \beta = \dfrac{8-10v_{out}}{15\left(1-v_{out}\right)}, v_{out} = \dfrac{\left(3K_{out} - 2G_{out}\right)}{2\left(3K_{out} + G_{out}\right)}$. For the case of fully random distribution of CNTs, i.e., no agglomeration occurs in the matrix phase, the effective elastic moduli K and G predicted by the M-T method are [1]

$$
K = K_m + \frac{V_{CNT}\left(\delta_r - 3K_m\alpha_r\right)}{3\left(c_m + V_{CNT}\alpha_r\right)},\quad
G = G_m + \frac{V_{CNT}\left(\eta_r - 2G_m\beta_r\right)}{2\left(c_m + V_{CNT}\beta_r\right)},
$$

where $c_m = 1 - V_{CNT}$. The effective elastic modulus (E) and Poisson's ratio (v) of the microbeam are calculated as

$$
E = \frac{9KG}{3K + G},\quad v = \frac{3K - 2G}{6K + 2G}.
$$

Meanwhile, the mixing rule is applied for the mass density as [12]

$$\rho = (\rho_{CNT} - \rho_m)\, V_{CNT} + \rho_m,$$

with ρ_{CNT}, ρ_m are, respectively, the density of the CNT reinforcement and the polymer matrix.

2.2. Strain energy

The elastic strain (U) of an elastic solid with a region V evaluated by the MCST is as follows [7]

$$U = \frac{1}{2}\int_V (\boldsymbol{\sigma} : \boldsymbol{\varepsilon} + \mathbf{m} : \boldsymbol{\chi})\, \mathrm{d}V = \frac{1}{2}\int_V \left(\sigma_{ij}\varepsilon_{ij} + m_{ij}\chi_{ij}\right) \mathrm{d}V, \quad i,j = 1,2,3 \tag{3}$$

where $\boldsymbol{\sigma}$ is the stress tensor; $\boldsymbol{\varepsilon}$ is the strain tensor, $\boldsymbol{\chi}$ is the symmetric curvature tensor, and $\mathbf{m}$ is the deviatoric part of the couple stress. These tensors are defined as follows

$$\begin{aligned}
&\boldsymbol{\varepsilon} = \frac{1}{2}\left[\nabla \mathbf{u} + (\nabla \mathbf{u})^T\right] && \text{or} && \varepsilon_{ij} = \frac{1}{2}\left(u_{i,j} + u_{j,i}\right),\\
&\boldsymbol{\sigma} = \lambda \mathrm{tr}\left(\boldsymbol{\varepsilon}\right) I + 2G\boldsymbol{\varepsilon} && \text{or} && \sigma_{ij} = \lambda\varepsilon_{kk}\delta_{ij} + 2G\varepsilon_{ij},\\
&\boldsymbol{\chi} = \frac{1}{2}\left[\nabla \boldsymbol{\theta} + (\nabla \boldsymbol{\theta})^T\right] && \text{or} && \chi_{ij} = \frac{1}{2}\left(\theta_{i,j} + \theta_{j,i}\right),\\
&\mathbf{m} = 2l^2 G\boldsymbol{\chi} && \text{or} && m_{ij} = 2l^2 G\chi_{ij}.
\end{aligned} \tag{4}$$

In the above equation, $\mathbf{u}$ denotes the vector of displacements; l is the material-length-scale parameter; $\boldsymbol{\theta} = \frac{1}{2}\mathrm{curl}\left(\mathbf{u}\right)$ or $\theta_i = \frac{1}{2}e_{ijk}u_{k,j}$ is the rotation vector, and λ, G are the Lame's constants.

2.3. Mathematical formulation

According to the refined third-order shear deformation theory [13], displacements of a point inside the microbeam in the x- and z-directions, $u(x,z,t), w(x,z,t)$, respectively, are given by

$$u = u_0(x,t) + \frac{z}{4}(5\phi + w_{0,x}) - \frac{5z^3}{3h^2}(\phi + w_{0,x}), \quad w = w_0(x,t), \tag{5}$$

where $u_0\left(x,t\right), w_0\left(x,t\right)$ denote the longitudinal and transversal displacements of a point on the x-axis; ϕ is the sectional rotation. In Eq. (5), the subscript comma denotes the derivative with respect to the variable that follows.

Traditionally, the beam deformation is expressed in terms of three variables such as u, w, ϕ. However, to improve the effectiveness of the finite element formulation which will be derived later, this study employs the transverse shear rotation γ_0, defined as $\gamma_0 =$

$\phi + w_{0,x}$ to replace the rotation ϕ. Using the transverse shear rotation, one can rewrite the displacement field in (5) as follows

$$u = u_0(x,t) + z\left(\frac{5}{4}\gamma_0 - w_{0,x}\right) - \frac{5z^3}{3h^2}\gamma_0, \quad w = w_0(x,t). \tag{6}$$

From Eqs. (4) and (6), one can obtain the normal and shear strains in the form

$$\begin{aligned} \varepsilon_{xx} &= u_{,x} = u_{0,x} + z\left(\frac{5}{4}\gamma_{0,x} - w_{0,xx}\right) - \frac{5z^3}{3h^2}\gamma_{0,x}, \\ \gamma_{xz} &= u_{,z} + w_{,x} = 5\left(\frac{1}{4} - \frac{1}{h^2}z^2\right)\gamma_0. \end{aligned} \tag{7}$$

The rotation vectors are obtained as follows

$$\begin{aligned} \theta_y &= \frac{1}{2}\left(u_{,z} - w_{,x}\right) = \frac{1}{2}\left(\frac{5}{4}\gamma_0 - \frac{5}{h^2}\gamma_0 z^2 - 2w_{0,x}\right), \\ \theta_x &= \frac{1}{2}\left(w_{,y} - v_{,z}\right) = 0, \\ \theta_z &= \frac{1}{2}\left(v_{,x} - u_{,y}\right) = 0. \end{aligned}$$

Then, the symmetric curvature tensors are calculated through the rotation vectors

$$\begin{aligned} \chi_{xy} &= \frac{1}{2}\left(\theta_{x,y} + \theta_{y,x}\right) = \frac{1}{4}\left(\frac{5}{4}\gamma_{0,x} - \frac{5}{h^2}\gamma_{0,x}z^2 - 2w_{0,xx}\right), \\ \chi_{yz} &= \frac{1}{2}\left(\theta_{z,y} + \theta_{y,z}\right) = -\frac{5}{2h^2}\gamma_0 z, \\ \chi_{xx} &= \chi_{yy} = \chi_{zz} = \chi_{zx} = 0. \end{aligned} \tag{8}$$

The classical and couple stresses for the CNTRC microbeams are expressed as

$$\sigma_{xx} = E\varepsilon_{xx}, \quad \tau_{xz} = G\,\gamma_{xz}, \quad m_{xy} = m_{yx} = 2Gl^2\chi_{xy}, \quad m_{yz} = m_{zy} = 2Gl^2\chi_{yz}. \tag{9}$$

By inserting Eqs. (7), (8), and (9) into Eq. (3), the strain energy of the microbeams can be given as

$$\begin{aligned} U &= \frac{1}{2}\int_V \left(\sigma_{xx}\varepsilon_{xx} + \tau_{xz}\gamma_{xz} + 2m_{xy}\chi_{xy} + 2m_{yz}\chi_{yz}\right)\mathrm{d}V \\ &= \frac{1}{2}\int_0^L \Bigg[A_{11}u_{0,x}^2 + 2A_{12}u_{0,x}\left(\frac{5}{4}\gamma_{0,x} - w_{0,xx}\right) + A_{22}\left(\frac{5}{4}\gamma_{0,x} - w_{0,xx}\right)^2 - \frac{10}{3h^2}A_{34}u_{0,x}\gamma_{0,x} \\ &\quad - \frac{10}{3h^2}A_{44}\gamma_{0,x}\left(\frac{5}{4}\gamma_{0,x} - w_{0,xx}\right) + \frac{25}{9h^4}A_{66}\gamma_{0,x}^2 + 25\left(\frac{1}{16}B_{11} - \frac{1}{2h^2}B_{22} + \frac{1}{h^4}B_{44}\right)\gamma_0^2 \\ &\quad + C_{11}\left(\frac{5}{8}\gamma_{0,x} - w_{0,xx}\right)^2 - C_{22}\frac{5}{h^2}\gamma_{0,x}\left(\frac{5}{8}\gamma_{0,x} - w_{0,xx}\right) + C_{22}\frac{25}{h^4}\gamma_0^2 + C_{44}\frac{25}{4h^4}\gamma_{0,x}^2\Bigg]\mathrm{d}x \end{aligned} \tag{10}$$

where $A_{11}, A_{12}, \ldots, A_{66}, B_{11}, B_{22}, B_{44}$ and C_{11}, C_{22}, C_{44} are the rigidity coefficients, defined as

$$(A_{11}, A_{12}, A_{22}, A_{34}, A_{44}, A_{66}) = bE \int_{-h/2}^{h/2} \left(1, z, z^2, z^3, z^4, z^6\right) \mathrm{d}z,$$

$$(B_{11}, B_{22}, B_{44}) = bG \int_{-h/2}^{h/2} \left(1, z^2, z^4\right) \mathrm{d}z,$$

$$(C_{11}, C_{22}, C_{44}) = bGl^2 \int_{-h/2}^{h/2} \left(1, z^2, z^4\right) \mathrm{d}z.$$

The kinetic energy T is calculated as

$$\begin{aligned} T &= \frac{1}{2} \int_0^L \int_A \rho \left(\dot{u}^2 + \dot{w}^2\right) \mathrm{d}A \mathrm{d}x \\ &= \frac{1}{2} \int_0^L \left[I_{11} \left(\dot{u}_0^2 + \dot{w}_0^2\right) + 2 I_{12} \dot{u}_0 \left(\frac{5}{4}\dot{\gamma}_0 - \dot{w}_{0,x}\right) + I_{22} \left(\frac{5}{4}\dot{\gamma}_0 - \dot{w}_{0,x}\right)^2 \right. \\ &\quad \left. - \frac{10}{3h^2} I_{34} \dot{u}_0 \dot{\gamma}_0 - \frac{10}{3h^2} I_{44} \dot{\gamma}_0 \left(\frac{5}{4}\dot{\gamma}_0 - \dot{w}_{0,x}\right) + \frac{25}{9h^4} I_{66} \dot{\gamma}_0^2 \right] \mathrm{d}x \end{aligned} \tag{11}$$

with $I_{11}, I_{12}, \ldots, I_{66}$ are the moments of mass and they are defined as

$$(I_{11}, I_{12}, I_{22}, I_{34}, I_{44}, I_{66}) = b \int_{-h/2}^{h/2} \rho \left(1, z, z^2, z^3, z^4, z^6\right) \mathrm{d}z.$$

Note that the over dot in Eq. (11) and in the below denotes the derivative with respect to time.

The potential of the moving load (V) is of the form

$$V = -\int_0^L P w_0(x,t) \delta\left(x - vt\right) \mathrm{d}x,$$

where $\delta(.)$ is the delta Dirac function; x is the abscissa of the moving load, measured from the left support.

3. BEAM ELEMENT FORMULATION

A two-node beam element with length a is considered. The vector of nodal degrees of freedom ($\mathbf{d}$) for the element is of the form

$$\mathbf{d} = \{\mathbf{d}_u \ \mathbf{d}_w \ \mathbf{d}_\gamma\}^T, \tag{12}$$

where

$$\mathbf{d}_u = \{u_{01} \ u_{02}\}^T, \ \ \mathbf{d}_w = \{w_{01} \ w_{0x1} \ w_{02} \ w_{0x2}\}^T, \ \ \mathbf{d}_\gamma = \{\gamma_{01} \ \gamma_{02}\}^T, \tag{13}$$

are, respectively, the vectors of values of u_0, w_0 and γ_0 at the two nodes. The superscript 'T' in Eqs. (12), (13), and in the below implies the transpose of a vector or a matrix. The Lagrange and cubic Hermite functions are used to interpolate the displacements and shear rotation, specifically as follows

$$u_0 = \mathbf{N}\mathbf{d}_u, \quad w_0 = \mathbf{H}\mathbf{d}_w, \quad \gamma_0 = \mathbf{N}\mathbf{d}_\gamma,$$

where $\mathbf{N} = \{N_1 \ N_2\}$, $\mathbf{H} = \{H_1 \ H_2 \ H_3 \ H_4\}$ in which

$$N_1 = 1 - \frac{x}{a}, \ N_2 = \frac{x}{a},$$
$$H_1 = 1 - 3\left(\frac{x}{a}\right)^2 + 2\left(\frac{x}{a}\right)^3, \ H_2 = x - 2\frac{x^2}{a} + \frac{x^3}{a^2},$$
$$H_3 = 3\left(\frac{x}{a}\right)^2 - 2\left(\frac{x}{a}\right)^3, \ H_4 = -\frac{x^2}{a} + \frac{x^3}{a^2}.$$

With the interpolations, the strain energy in Eq. (10) is rewritten as follows

$$U = \frac{1}{2}\sum^{ne} \mathbf{d}^T\mathbf{k}\mathbf{d} \quad \text{with} \quad \mathbf{k} = \begin{bmatrix} \mathbf{k}_{uu} & \mathbf{k}_{uw} & \mathbf{k}_{u\gamma} \\ \mathbf{k}_{uw}^T & \mathbf{k}_{ww} & \mathbf{k}_{w\gamma} \\ \mathbf{k}_{u\gamma}^T & \mathbf{k}_{w\gamma}^T & \mathbf{k}_{\gamma\gamma} \end{bmatrix}, \tag{14}$$

with ne is the total number of elements; $\mathbf{k}$ is the element stiffness matrix. In Eq. (14), $\mathbf{k}_{uu}, \mathbf{k}_{uw}, \ldots, \mathbf{k}_{\gamma\gamma}$ are the stiffness sub-matrices due to the axial stretching, bending, shear deformation and their couplings. These sub-matrices are as follows

$$\mathbf{k}_{uu} = \int_0^a \mathbf{N}_{,x}^T A_{11}\mathbf{N}_{,x}\mathrm{d}x, \quad \mathbf{k}_{ww} = \int_0^a \mathbf{H}_{,xx}^T \left(A_{22} + C_{11}\right)\mathbf{H}_{,xx}\mathrm{d}x,$$

$$\mathbf{k}_{uw} = -2\int_0^a \mathbf{N}_{,x}^T A_{12}\mathbf{H}_{,xx}\mathrm{d}x, \quad \mathbf{k}_{u\gamma} = 5\int_0^a \left(\frac{1}{2}\mathbf{N}_{,x}^T A_{12}\mathbf{N}_{,x} - \frac{2}{3h^2}\mathbf{N}_{,x}^T A_{34}\mathbf{N}_{,x}\right)\mathrm{d}x,$$

$$\mathbf{k}_{w\gamma} = 5\int_0^a \left(-\frac{1}{2}\mathbf{H}_{,xx}^T A_{22}\mathbf{N}_{,x} + \frac{2}{3h^2}\mathbf{H}_{,xx}^T A_{44}\mathbf{N}_{,x} - \frac{1}{4}\mathbf{H}_{,xx}^T C_{11}\mathbf{N}_{,x} + \frac{1}{h^2}\mathbf{H}_{,xx}^T C_{22}\mathbf{N}_{,x}\right)\mathrm{d}x,$$

$$\mathbf{k}_{\gamma\gamma} = 25\int_0^a \left[\frac{1}{16}\mathbf{N}_{,x}^T A_{22}\mathbf{N}_{,x} - \frac{1}{6h^2}\mathbf{N}_{,x}^T A_{44}\mathbf{N}_{,x} + \frac{1}{9h^4}\mathbf{N}_{,x}^T A_{66}\mathbf{N}_{,x} + \mathbf{N}^T\left(\frac{1}{16}B_{11} - \frac{1}{2h^2}B_{22} + \frac{1}{h^4}B_{44}\right)\mathbf{N} + \frac{1}{64}\mathbf{N}_{,x}^T C_{11}\mathbf{N}_{,x} - \frac{1}{8h^2}\mathbf{N}_{,x}^T C_{22}\mathbf{N}_{,x} + \frac{1}{4h^4}\mathbf{N}_{,x}^T C_{44}\mathbf{N}_{,x} + \frac{1}{h^4}\mathbf{N}^T C_{22}\mathbf{N}\right]\mathrm{d}x.$$

The kinetic energy in Eq. (11) can also be written as

$$T = \frac{1}{2}\sum^{ne}\dot{\mathrm{d}}^T\mathbf{m}\dot{\mathrm{d}} \quad \text{with} \quad \mathbf{m} = \begin{bmatrix} \mathbf{m}_{uu} & \mathbf{m}_{uw} & \mathbf{m}_{u\gamma} \\ \mathbf{m}_{uw}^T & \mathbf{m}_{ww} & \mathbf{m}_{w\gamma} \\ \mathbf{m}_{u\gamma}^T & \mathbf{m}_{w\gamma}^T & \mathbf{m}_{\gamma\gamma} \end{bmatrix}, \tag{15}$$

with $\mathbf{m}$ denotes the mass matrix of the element. The sub-matrices in Eq. (15) have the following forms

$$\mathbf{m}_{uu} = \int_0^a \mathbf{N}^T I_{11}\mathbf{N}\mathrm{d}x, \quad \mathbf{m}_{ww} = \int_0^a \left(\mathbf{H}^T I_{11}\mathbf{H} + \mathbf{H}_{,x}^T I_{22}\mathbf{H}_{,x}\right)\mathrm{d}x,$$

$$\mathbf{m}_{uw} = -\int_0^a \mathbf{N}^T I_{12}\mathbf{H}_{,x}\mathrm{d}x, \quad \mathbf{m}_{u\gamma} = 5\int_0^a \left(\frac{1}{4}\mathbf{N}^T I_{12}\mathbf{N} - \frac{1}{3h^2}\mathbf{N}^T I_{34}\mathbf{N}\right)\mathrm{d}x,$$

$$\mathbf{m}_{w\gamma} = 5\int_0^a \left(-\frac{1}{4}\mathbf{H}_{,x}^T I_{22}\mathbf{N} + \frac{1}{3h^2}\mathbf{H}_{,x}^T I_{44}\mathbf{N}\right)\mathrm{d}x,$$

$$\mathbf{m}_{\gamma\gamma} = 25\int_0^a \mathbf{N}^T\left(\frac{1}{16}I_{22} - \frac{1}{2h^2}I_{44} + \frac{1}{h^4}I_{66}\right)\mathbf{N}\mathrm{d}x.$$

The governing equation for vibration analysis of the micro-scale beam can be established by using the derived element stiffness and mass matrices

$$\mathbf{M}\ddot{\mathbf{D}} + \mathbf{K}\mathbf{D} = \mathbf{F}^{\mathrm{ex}}, \tag{16}$$

where $\mathbf{D}$, $\mathbf{M}$, and $\mathbf{K}$ are the global vector of nodal displacements, the mass and stiffness matrices, respectively; $\mathbf{F}^{\mathrm{ex}}$ is the global vector of nodal external load with the form

$$\mathbf{F}^{\mathrm{ex}} = \left\{0\ 0\ldots\ 0\ 0 \quad \underbrace{PH_1|_{x_e}\ldots PH_4|_{x_e}}_{\text{element under loading}} \quad 0\ 0\ldots 0\ 0\right\}^T_{x_e}. \tag{17}$$

Note that only the coefficients corresponding to the element under loading of the vector $\mathbf{F}^{\text{ex}}$ are nonzero, and the notation $H_1|_{x_e} \dots H_4|_{x_e}$ in Eq. (17) means that the functions H_i $(i = 1, \dots, 4)$ are evaluated at the x_e, the current abscissa of the load P with respect to the left node of the element. Eq. (16) is solved herein by the implicit Newmark method, namely the average acceleration method.

For the free vibration analysis, the right side of Eq. (16) is set to $\mathbf{0}$, which leads to

$$\mathbf{M}\ddot{\mathbf{D}} + \mathbf{K}\mathbf{D} = \mathbf{0}. \tag{18}$$

Assuming a harmonic response, and Eq. (18) leads to the following eigenvalue problem

$$\left(\mathbf{K} - \omega^2\mathbf{M}\right)\bar{\mathbf{D}} = \mathbf{0}, \tag{19}$$

with ω is the circular frequency, $\bar{\mathbf{D}}$ is the vibration amplitude. The solution of Eq. (19) gives the natural frequencies of the microbeam.

4. NUMERICAL APPLICATION

The derived formulations are applied to vibration analysis of a CNTRC microbeam with simply supported ends. To this end, the following data are used for the matrix and reinforcement: $E_m = 2.5\,\text{GPa}, \rho_m = 1190\,\text{kg/m}^3, \nu_m = 0.3$, $\rho_{CNT} = 1400\,\text{kg/m}^3$ and elastic constants listed in Table 1. The height of the microbeam is taken as $h = 1\text{e}{-9}$ m; a moving load $P = \rho_m ALg$ with $g = 9.81\,\text{m/s}^2$ is employed. The fundamental frequency parameter is normalized by $\lambda = \omega L\sqrt{I_{110}/A_{110}}$ where A_{110} and I_{110} are the values of A_{11} and I_{11} of microbeam made of pure matrix material, respectively. The dynamic factor D_d is defined as $D_d = \max\left(\dfrac{w\,(L/2,t)}{w_{st}}\right)$, where $w_{st} = PL^3/48E_mI$ is the maximum deflection of a pure polymer microbeam under static load $P = \rho_m ALg$ (with $I = bh^3/12$). The Newmark method is performed herein for a time step $\Delta t = \Delta T/200$, where ΔT is the time needed for the load to cross the microbeam.

Table 1. The Hill elastic coefficients of CNTs [12]

Radius (A°)	k_r (GPa)	l_r (GPa)	m_r (GPa)	n_r (GPa)	p_r (GPa)
10	30	10	1	450	1

4.1. Accuracy and convergence

Before conducting numerical calculations, the accuracy and convergence of the derived formula are studied. Table 2 compares the frequency parameters of homogeneous microbeams made from SiC and Al with $l = 17.6\,\mu\text{m}; h/l = 2.0$ and $L/h = 10$. Material properties for Al and SiC are given in [4].

Table 2. Convergence of element in predicting frequency parameters of homogeneous microbeam

Material	Present						Ref. [4]	Error (%)
	$ne = 2$	$ne = 4$	$ne = 6$	$ne = 8$	$ne = 10$	$ne = 20$		
SiC	0.8492	0.8461	0.8459	0.8459	0.8459	0.8459	0.8336	1.48
Al	0.3576	0.3562	0.3562	0.3561	0.3561	0.3561	0.3393	4.95

It is found that the results predicted by the present formulation are quite close to that of Ref. [4]. The small difference can be explained by the different beam theories used in the two works (the Timoshenko beam theory is used in Ref. [4]). A rapid convergence of the derived beam element in determining the frequency parameters of the micro-scale beam is also seen in Table 2.

Table 3. Convergence of element in predicting frequency parameters of randomly oriented CNTRC microbeam

Present						Ref. [14]	Error (%)
$ne = 2$	$ne = 4$	$ne = 6$	$ne = 8$	$ne = 10$	$ne = 20$		
3.4491	3.4428	3.4424	3.4423	3.4423	3.4423	3.574603	3.84

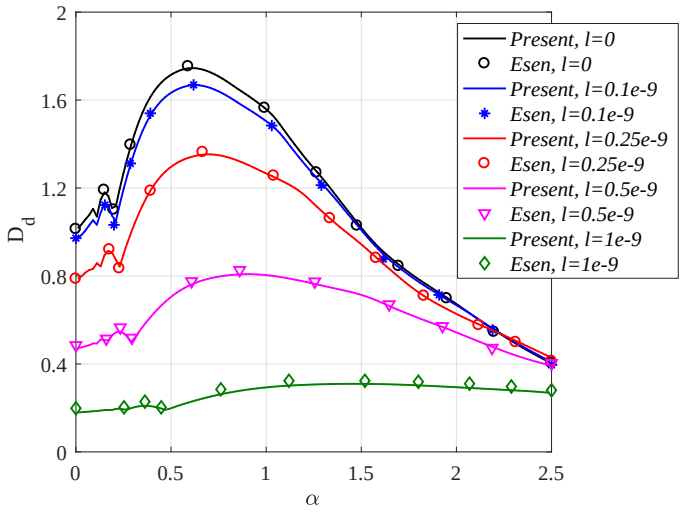

Fig. 2. Comparison of the dynamic factor of homogeneous microbeam under a moving load

Table 3 shows the convergence of the derived beam element in predicting the frequency parameter of a randomly oriented CNTRC microbeam with $V_{CNT} = 0.075$. Similar to Table 2, a mesh of only 8 elements is required for predicting the frequencies. It is

worth noting that Yas and Heshmati [14] need 100 Timoshenko beam elements. The error in the frequency parameters of the two works can also arise from the different theories adopted in the two works and the effect of CNT agglomeration is ignored in Ref. in [14]. With this convergence result, a mesh of 8 elements is employed in the below.

Fig. 2 compares the dynamic magnification factor (DMF) of homogeneous microbeam under a moving load obtained in the present work with that of Esen [11] for various values of the size scale parameter l. The speed parameter α is defined in accordance with Ref. [11]. A good agreement between the DMF of the present work and that of Ref. [11] is noted in Fig. 2. A finite element formulation derived from Timoshenko beam theory was used to predict the DMF in Ref. [11].

4.2. Free vibration

Table 4 lists the frequency parameters of the CNTRC microbeam with an aspect ratio $L/h = 20$ for $\zeta = 1$ and different values of the ξ, V_{CNT} and l. According to the results obtained previously, the stiffness of the microbeam increases as the volume fraction of CNT increases. However, the frequency parameter in Table 4 is not expected to increase by increasing the V_{CNT}. The frequency parameters of the microbeam increase sharply only when CNTs agglomeration does not occur ($\zeta = \xi = 1$). On the contrary, when CNTs agglomeration is severe, e.g. $\zeta = 1, \xi = 0.1$, a small amount of CNTs reinforcement will help increase the frequency parameters of the microbeam. On the other hand, when the amount of CNTs reinforcement is greater, the frequency parameter does not increase, even it decreases. This phenomenon does not depend on the value of the size scale parameter l. Table 4 also shows the significant influence of the size scale parameter on the frequencies of the micro-scale beam. The frequencies are enhanced by

Table 4. The frequency parameters of microbeam for $\zeta = 1$ and different values of ξ, V_{CNT} and l

	$\zeta = 1$	$V_{CNT} = 0$	$V_{CNT} = 0.02$	$V_{CNT} = 0.05$	$V_{CNT} = 0.1$	$V_{CNT} = 0.2$	$V_{CNT} = 0.3$
$l = 0$	$\xi = 0.1$	0.1419	0.1529	0.1546	0.1548	0.1540	0.1529
	$\xi = 0.5$	0.1419	0.1714	0.1931	0.2097	0.2221	0.2263
	$\xi = 1$	0.1419	0.1792	0.2237	0.2826	0.3735	0.4462
$l = 0.25\text{e}{-9}$	$\xi = 0.1$	0.1611	0.1737	0.1757	0.1759	0.1750	0.1737
	$\xi = 0.5$	0.1611	0.1949	0.2196	0.2385	0.2526	0.2575
	$\xi = 1$	0.1611	0.2038	0.2545	0.3216	0.4247	0.5069
$l = 0.5\text{e}{-9}$	$\xi = 0.1$	0.2084	0.2249	0.2274	0.2278	0.2265	0.2249
	$\xi = 0.5$	0.2084	0.2525	0.2847	0.3093	0.3277	0.3340
	$\xi = 1$	0.2084	0.2641	0.3302	0.4172	0.5504	0.6560
$l = 1\text{e}{-9}$	$\xi = 0.1$	0.3368	0.3635	0.3677	0.3682	0.3663	0.3636
	$\xi = 0.5$	0.3368	0.4084	0.4608	0.5008	0.5306	0.5409
	$\xi = 1$	0.3368	0.4273	0.5347	0.6757	0.8907	1.0602

increasing the parameter l, regardless of the CNT volume fraction and the agglomeration parameters as well.

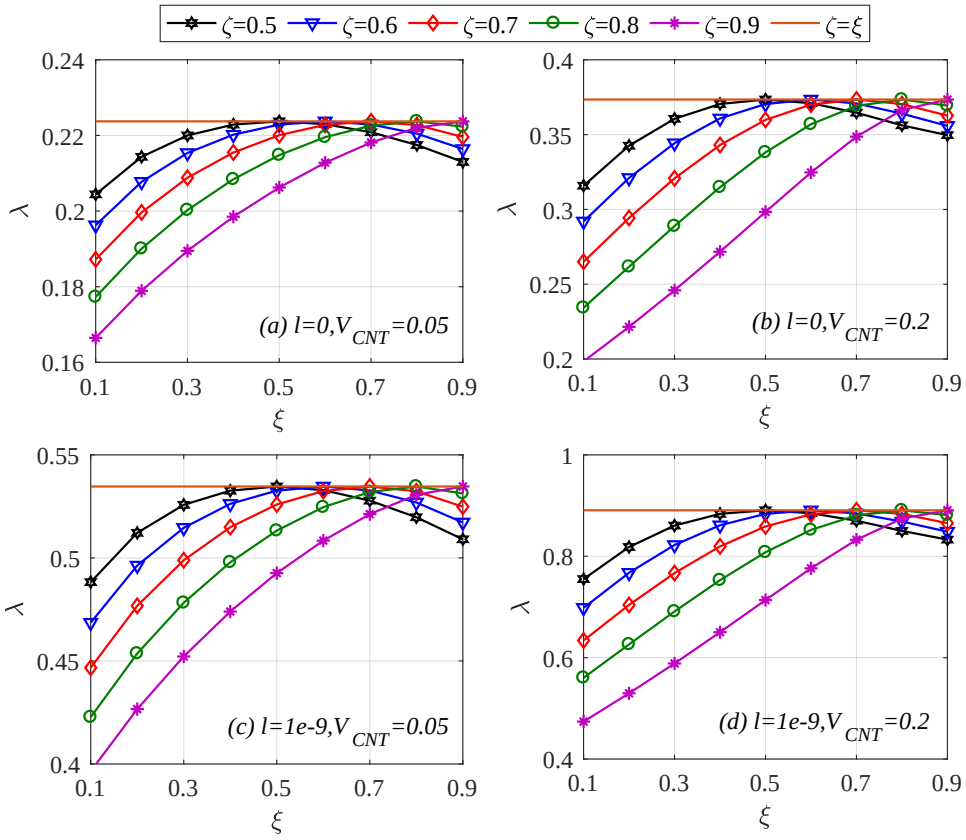

Fig. 3. Effects of agglomeration parameters on the frequency parameter of the microbeam

The effects of the agglomeration parameters on the frequency parameter of the microbeam are shown in Fig. 3. From the figure one sees that in the case $\xi < \zeta$, the increase of the parameter ξ enhances the frequency parameter, and the frequency parameter attains the highest value when $\xi = \zeta$, which is the uniform distribution of CNTs. On the other hand, when $\xi > \zeta$, the frequency parameter is decreased by increasing the parameter ξ. The figure also shows the frequency parameter is enhanced by the increase of the size scale parameter l.

4.3. Dynamic response

This subsection studies the influence of various parameters on the dynamic behavior of the CNTRC microbeams. In Fig. 4, the relations between the DMF and the speed v of the CNTRC microbeam are illustrated for $V_{CNT} = 0.02$ and $V_{CNT} = 0.2$. Two pairs of the

agglomeration parameters, $(\zeta, \xi) = (1, 0.1)$ and $(1, 1)$ and different values of the size scale parameter l are considered in the figure. One can see from the figure that the increase of the parameter l results in a significant decrease in the DMF, regardless of the V_{CNT} as well as agglomeration parameters. This phenomenon can be explained by the fact that the strain energy evaluated by the MCST is larger, and this leads to higher stiffness. As a result, the DMF is decreased by the increase of the microbeam stiffness. In addition, the DMF has a lower value corresponding to microbeams without CNT agglomeration $(\zeta = \xi = 1)$, this is seen more clearly when the V_{CNT} value is larger (comparing Fig. 4(d) with Fig. 4(c)). An increase in the CNT reinforcement helps to reduce the DMF, by this is clearly seen only when CNTs are not agglomerated $(\zeta = \xi = 1)$. In the case of severe agglomeration of CNTs, the increase of the CNT reinforcement does not seem to have much effect (comparing Fig. 4(c) with Fig. 4(a)). In addition, the effect of the moving load speed on the factor D_d of the CNTRC microbeams is similar to that of conventional beams, that is the factor D_d experiences a repeatedly increasing and decreasing period when the load speed is low, it then increases to a peak value before decreases gradually.

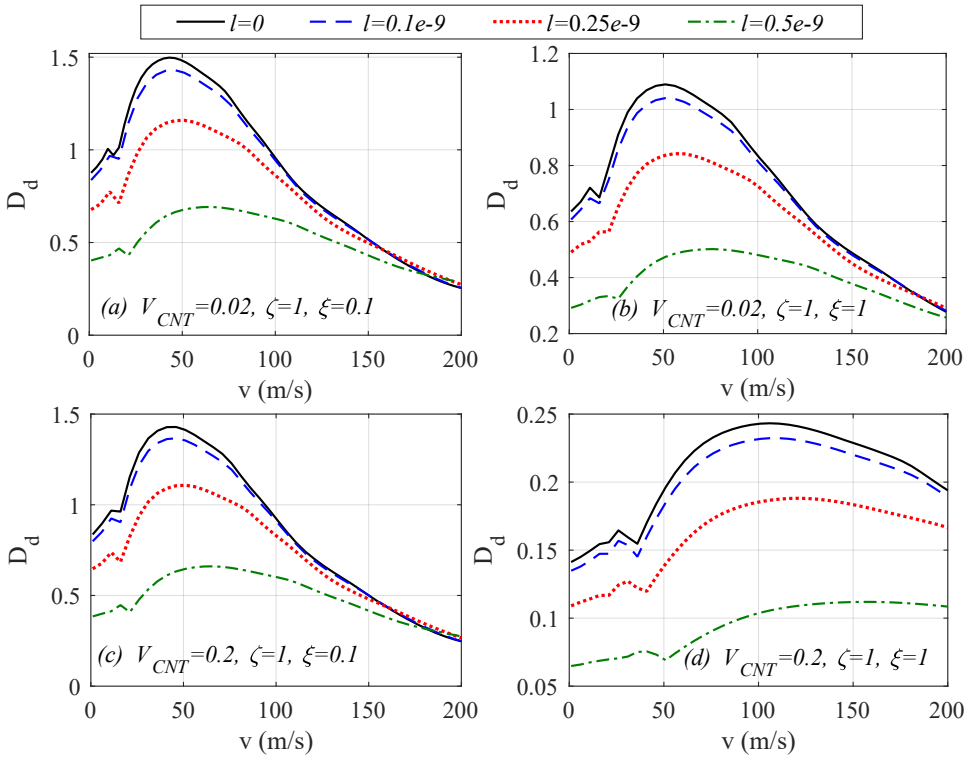

Fig. 4. Relations between the DMF and the moving load speed of CNTRC microbeam with different size scale parameters

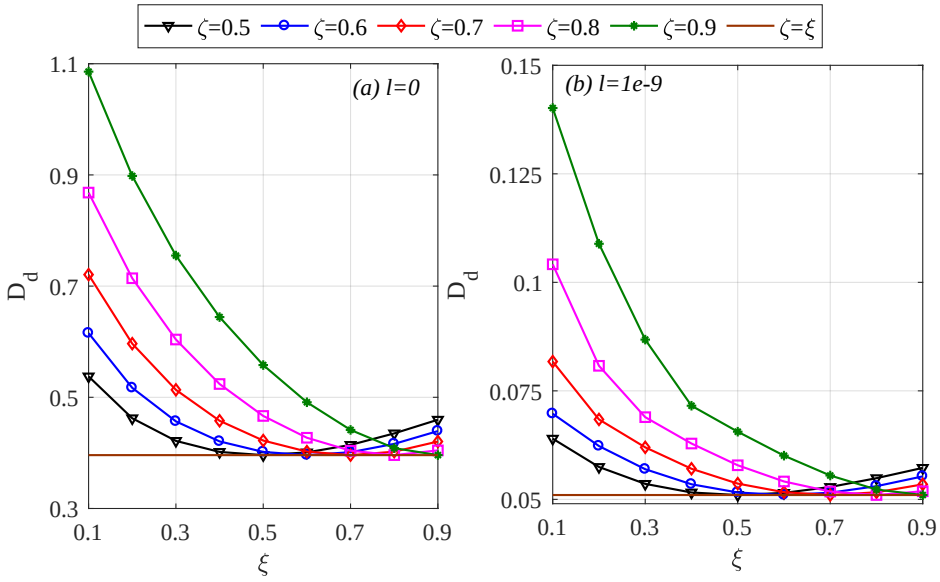

Fig. 5. Variation of the dynamic factor with parameter ξ for $V_{CNT} = 0.1$, $v = 50$ m/s and various values of parameter ζ

The dependence of the factor D_d upon the two agglomeration parameters is further shown in Fig. 5 for $V_{CNT} = 0.1$, $v = 50$ m/s. From the figure, one can see that in the case $\xi < \zeta$, the factor D_d declines by increasing the parameter ξ, and it reaches the lowest value when $\xi = \zeta$, that is when the CNTs are uniformly distributed. For the $\xi > \zeta$, the factor D_d increases again by the increase of the parameter ξ. The influence of the size scale parameter l on the factor D_d is also clearly observed in the figure, where the factor D_d is considerably lower for the microbeam associated with a higher value of the parameter l.

5. CONCLUSIONS

The vibration analysis of micro-scale CNTRC beams carrying a moving concentrated load was studied in the framework of the MCST and a refined high-order beam theory. The effect of CNTs agglomeration is considered by using the Mori–Tanaka method to estimate the effective elastic moduli of CNTRC. The mathematical model of the microbeam is established in terms of the transverse shear rotation. The discretized governing equation for the microbeams is constructed with the help of a finite beam element, and solved by an implicit direct integration method. The effects of the CNT reinforcement, the agglomeration, the size scale parameter, and the loading speed on the vibration have been numerically examined in detail. Some main conclusions drawn from this work are as follows:

- The frequencies of the microbeam are enhanced by the CNT reinforcement, but the enhancement is dependent on the degree of agglomeration of the CNTs. If the CNTs agglomeration does not occur, the frequency parameter increases sharply when the microbeam is reinforced by higher CNT volume fraction. However, if CNTs agglomeration becomes serious, more CNTs reinforcement does not enhance the frequency parameter of the microbeam.

- The microstructural size effect has an important role of the frequencies of the microbeam, and an increase in the size scale parameter leads to an increase in the frequency parameter. On the other hand, the DMF tends to decrease when increasing the value of the scale parameter.

- DMF decreases by the CNT reinforcement, but this decrease depends on the degree of the CNT agglomeration. When the CNTs agglomeration becomes severe, the increase of the CNT volume fraction hardly decreases the dynamic factor of the CNTRC microbeam.

DECLARATION OF COMPETING INTEREST

The authors declare that they have no known competing financial interests or personal relationships that could have appeared to influence the work reported in this paper.

ACKNOWLEDGMENT

This research was supported by a research fund from the Institute of Mechanics, VAST (Vietnam) under the grand number VCH.TX.05/2024.

REFERENCES

[1] D.-L. Shi, X.-Q. Feng, Y. Y. Huang, K.-C. Hwang, and H. Gao. The effect of nanotube waviness and agglomeration on the elastic property of carbon nanotube-reinforced composites. *Journal of Engineering Materials and Technology*, **126**, (2004), pp. 250–257. https://doi.org/10.1115/1.1751182.

[2] M. Heshmati and M. H. Yas. Free vibration analysis of functionally graded CNT-reinforced nanocomposite beam using Eshelby-Mori-Tanaka approach. *Journal of Mechanical Science and Technology*, **27**, (2013), pp. 3403–3408. https://doi.org/10.1007/s12206-013-0862-8.

[3] T. T. Tran and D. K. Nguyen. Dynamics of inclined CNTRC sandwich beams under a moving mass with influence of CNT agglomeration. *Comptes Rendus. Mécanique*, **351**, (2023), pp. 373–390. https://doi.org/10.5802/crmeca.226.

[4] L.-L. Ke and Y.-S. Wang. Size effect on dynamic stability of functionally graded microbeams based on a modified couple stress theory. *Composite Structures*, **93**, (2011), pp. 342–350. https://doi.org/10.1016/j.compstruct.2010.09.008.

[5] R. A. Toupin. Elastic materials with couple-stresses. *Archive for Rational Mechanics and Analysis*, **11**, (1), (1962), pp. 385–414. https://doi.org/10.1007/bf00253945.

[6] R. D. Mindlin and H. F. Tiersten. Effects of couple-stresses in linear elasticity. *Archive for Rational Mechanics and Analysis*, **11**, (1), (1962), pp. 415–448. https://doi.org/10.1007/bf00253946.

[7] F. Yang, A. C. M. Chong, D. C. C. Lam, and P. Tong. Couple stress based strain gradient theory for elasticity. *International Journal of Solids and Structures*, **39**, (2002), pp. 2731–2743. https://doi.org/10.1016/s0020-7683(02)00152-x.

[8] M. Mohammadimehr, A. A. Monajemi, and H. Afshari. Free and forced vibration analysis of viscoelastic damped FG-CNT reinforced micro composite beams. *Microsystem Technologies*, **26**, (2017), pp. 3085–3099. https://doi.org/10.1007/s00542-017-3682-4.

[9] Ö. Civalek, S. Dastjerdi, Ş. D. Akbaş, and B. Akgöz. Vibration analysis of carbon nanotube-reinforced composite microbeams. *Mathematical Methods in the Applied Sciences*, (2021). https://doi.org/10.1002/mma.7069.

[10] D. M. R. Al-Shewailiah and M. A. Al-Shujairi. Static bending of functionally graded single-walled carbon nanotube conjunction with modified couple stress theory. *Materials Today: Proceedings*, **61**, (2022), pp. 1023–1037. https://doi.org/10.1016/j.matpr.2021.10.295.

[11] I. Esen. Dynamics of size-dependant Timoshenko micro beams subjected to moving loads. *International Journal of Mechanical Sciences*, **175**, (2020). https://doi.org/10.1016/j.ijmecsci.2020.105501.

[12] H. Daghigh and V. Daghigh. Free vibration of size and temperature-dependent carbon nanotube (CNT)-reinforced composite nanoplates with CNT agglomeration. *Polymer Composites*, **40**, (2018). https://doi.org/10.1002/pc.25057.

[13] G. Shi. A new simple third-order shear deformation theory of plates. *International Journal of Solids and Structures*, **44**, (2007), pp. 4399–4417. https://doi.org/10.1016/j.ijsolstr.2006.11.031.

[14] M. H. Yas and M. Heshmati. Dynamic analysis of functionally graded nanocomposite beams reinforced by randomly oriented carbon nanotube under the action of moving load. *Applied Mathematical Modelling*, **36**, (2012), pp. 1371–1394. https://doi.org/10.1016/j.apm.2011.08.037.